

# On O-X mode conversion in a cold magnetized 2D inhomogeneous plasma in the electron cyclotron frequency range

**A Yu Popov**

Ioffe Physico-Technical Institute, St.Petersburg, Russia

E-mail: a.popov@mail.ioffe.ru

## **Abstract.**

In this paper a reduced set of the partial differential wave equations valid in the conversion layer close to O-mode cutoff surface and accounting for the magnetic field 2D inhomogeneity with no restriction to an angle between the toroidal direction and the magnetic field direction is derived. An integral representation of a solution to the derived set of equation is given. For the particular case of small angle between O mode cut-off surface and X mode cut-off surface an explicit expressions for both the electric field components and the conversion coefficients are obtained and its properties are considered in details.

## 1. Introduction

Nowadays the electron Bernstein waves (EBWs) having no density cut-offs and effectively damped even at high electron cyclotron harmonics are considered as the most promising candidate to provide an auxiliary heating and current drive in a dense plasma of a spherical tokamaks and stellarators [1, 2, 3]. The EBW could be excited via direct conversion of X mode to Bernstein mode in a vicinity of the upper hybrid resonance (UHR) or via so-called O-X-B scheme. The efficiency of last scheme, as it was demonstrated theoretically [4, 5, 6] in the frame of 1D slab model, is determined by the efficiency of O to X mode conversion, which can reach 100 percent value at the certain parallel refractive index being constant in slab geometry. Due to, in a real spherical tokamak's configurations, where the poloidal inhomogeneity of the magnetic field is important, both the parallel refractive index is no longer constant and the components of the dielectric tensor are functions of two co-ordinates, an analysis of the full-wave equations in the frame of 2D model is important. The first attempt to consider 2D model of OX conversion has been undertaken a couple of years ago [7]. The main conclusion provided by author of [7] concerning the absence of the O mode reflection from the O-mode cut-off surface seems to be quite doubtful and lacks support from the last two papers devoted to this topic [8, 9]. Unfortunately, the OX mode conversion in [8] has been considered in the frame of the oversimplified model ignoring as it does both the poloidal magnetic field and, as result, varying of the parallel refractive index on the magnetic surface. These effects were taken into account in [9], where the explicit expressions for the OX and XO conversion coefficients have been obtained simultaneously with [8] but for  $\varphi = \arctan B_\theta/B_z \ll \pi$  ( $B_\theta$  and  $B_z$  are the poloidal and toroidal components of the magnetic field and  $\varphi$  is an angle between the toroidal direction and the magnetic field).

Unlike the assumption used in [9],  $\varphi \ll \pi$ , in spherical tokamak's plasma  $\varphi$  is no longer small as it is demonstrated in figure 1 for a typical MAST tokamak discharge. Therefore, straightforward using the results of [9], without mentioning paper [8], to describe OX conversion in spherical tokamaks seems to be overhasty. Because of the intensive efforts are paid to provide an auxiliary heating in spherical tokamaks using OXB scheme, calculation of the OX conversion coefficient in the realistic 2D model is of great interest. In this paper a reduced set of the partial differential wave equations valid in a vicinity of the O-mode cutoff and accounting for the magnetic field 2D inhomogeneity with no restriction to an angle between the toroidal direction and the magnetic field are derived. A solution to the reduced set of equations has been obtained and its properties are considered in details.

## 2. Physical model

There are three effects that remain beyond the scope of the present paper. We neglect, first, the curvature of the magnetic field line at the magnetic surface because of its

local radius  $R_f$  is considerably greater than the beam radius  $\rho$ , second, the curvature of the magnetic flux surfaces assuming high localization of the conversion region, third, the magnetic field shear which is not important for OX conversion [10]. We restrict ourselves to the case of not extremely strong plasma density inhomogeneity  $L_n$  when geometrical optics can be applied except possibly near cut-off layer or possibly mode conversion layer. One introduces two Cartesian co-ordinate systems  $(x, y, z)$  and  $(x, \zeta, \xi)$  with distances scaled in the units  $c/\omega$  and their origin located at the O-mode cut-off surface (figure 2). The co-ordinates  $x, y$  and  $z$  imitate the flux surface label, the poloidal and the toroidal co-ordinates, respectively, and axes  $\mathbf{e}_\zeta$  and  $\mathbf{e}_\xi$  are along the magnetic field and perpendicular to it on the O-mode cut-off surface, respectively (figure 3). The transformation from  $y, z$  components to  $\zeta, \xi$  components convenient to represent the Maxwellian equations is

$$\begin{aligned} y &= \cos(\varphi)\zeta + \sin(\varphi)\xi \\ z &= -\sin(\varphi)\zeta + \cos(\varphi)\xi. \end{aligned} \quad (1)$$

One introduces the set of the wave equations for a monochromatic wave  $\sim \exp(i\omega t)$  as

$$\nabla \times \nabla \times \mathbf{E} = \epsilon \mathbf{E}, \quad \epsilon = \begin{pmatrix} \epsilon_+ & 0 & 0 \\ 0 & \epsilon_- & 0 \\ 0 & 0 & \eta \end{pmatrix}, \quad \mathbf{E} = \begin{pmatrix} E_+ \\ E_- \\ E_\xi \end{pmatrix}, \quad (2)$$

where  $E_\pm = (E_x \pm iE_\zeta)/\sqrt{2}$ ,  $\epsilon_\pm = 1 - v/(1 \pm q)$ ,  $\eta = 1 - v$ ,  $v = \omega_{pe}^2/\omega^2$ ,  $q = |\omega_{ce}|/\omega$ ,  $\omega_{pe}$  and  $\omega_{ce}$  are electron Langmuir and cyclotron frequencies, respectively.

Since a domain in a vicinity of O-mode cut off surface beyond the tokamak mid-plane is of interest, one can expand the plasma parameters, namely density  $n(x)$  and magnetic field modulus  $B(x, y)$ , into the Taylor series at  $r_0$

$$\begin{aligned} n(x) &\simeq n_0(1 + x/L_n) \\ B(x, y) &\simeq B_0(1 + x/L_{bx} + y/L_{by}), \end{aligned} \quad (3)$$

where

$$\begin{aligned} 1/L_n, \rho/L_{by} &\ll 1, \\ L_n^{-1} = \partial \ln n_e / \partial x|_{r_0}, L_{by}^{-1} &= \partial \ln B / \partial y|_{r_0}, \end{aligned} \quad (4)$$

are parameters being the first order quantity ( $O(1)$ ) and

$$\begin{aligned} 1/L_{bx} &\ll 1, \\ L_{bx}^{-1} = \partial \ln B / \partial x|_{r_0} & \end{aligned} \quad (5)$$

is one being the second order quantity ( $O(2)$ ). In order to study the properties of the waves in the mode conversion region we keep in mind that the component  $E_-$  is small compared to two others  $E_- \sim (E_+, E_\xi)/L_n$  there. Omitting in (2) the terms being higher order quantity than the first one obtains

$$\begin{aligned} \left( \frac{\partial^2}{\partial \xi^2} + \frac{q_0}{1 + q_0} + \frac{x}{L_n} - \frac{y}{L_{by}} \right) E_+ + \frac{1}{\sqrt{2}} \left( \frac{\partial}{\partial x} + i \frac{\partial}{\partial \zeta} \right) \frac{\partial}{\partial \xi} E_\xi &= 0 \\ \frac{1}{\sqrt{2}} \left( \frac{\partial}{\partial x} - i \frac{\partial}{\partial \zeta} \right) \frac{\partial}{\partial \xi} E_+ - \frac{x}{L_n} E_\xi &= 0, \end{aligned} \quad (6)$$

Due to tokamak symmetry we may assume that the wave fields vary as  $\exp(in_z z)$ , where  $n_z$  being constant is large. We would like to construct a solution  $\mathbf{E} = (E_+, E_\xi)$  of the system (6). To this end we look to develop the integral representation for required solutions of Laplace integral type

$$\mathbf{E}(x, y, z) = \int_C \frac{dn_y}{2\pi} \int_{-\infty}^{\infty} \frac{dn_z}{2\pi} \exp(in_y y + in_z z) \mathbf{E}(x, n_y, n_z), \quad (7)$$

where  $\mathbf{E}(x, n_y, n_z)$  is assumed analytic in some domain and the path of integration in the  $n_y$  plane is such that the integrand vanishes rapidly at the ends of the contour  $C$  or at infinity. Next

$$\begin{aligned} \left( -n_\xi^2 + n^{opt2} + \frac{x}{L_n} - \frac{i}{L_{by}} \frac{\partial}{\partial n_y} \right) E_+ + \frac{in_\xi}{\sqrt{2}} \left( \frac{\partial}{\partial x} - n_\zeta \right) E_\xi &= 0 \\ \frac{in_\xi}{\sqrt{2}} \left( \frac{\partial}{\partial x} + n_\zeta \right) E_+ - \frac{x}{L_n} E_\xi &= 0, \end{aligned} \quad (8)$$

where  $n^{opt} = \sqrt{q_0/(1+q_0)}$  and

$$\begin{aligned} n_\zeta &= \cos(\varphi) n_y - \sin(\varphi) n_z \\ n_\xi &= \sin(\varphi) n_y + \cos(\varphi) n_z. \end{aligned} \quad (9)$$

We cannot easily deal with the system (8) as it stands after transformation, but recalling the conclusions of 1D theory [4, 5] that the effective conversion is possible if both  $n_\zeta \ll 0$   $O(1)$  and  $n_\xi \sim \pm n^{opt} O(0)$  we may reduce it to a simpler form. Expanding  $n_\xi$  around  $n^{opt}$  and  $n_\zeta$  around 0 we have found that  $n_y^0 = \sin(\varphi) n^{opt}$  and  $n_z^0 = \cos(\varphi) n^{opt}$ . Keeping in (8) terms being the first order quantity one has

$$\begin{aligned} \left( -2n^{opt} \delta n_\xi + \frac{x}{L_n} - \frac{i}{L_{by}} \frac{\partial}{\partial \delta n_y} \right) E_+ + \frac{in^{opt}}{\sqrt{2}} \left( \frac{\partial}{\partial x} - \delta n_\zeta \right) E_\xi &= 0 \\ \frac{in^{opt}}{\sqrt{2}} \left( \frac{\partial}{\partial x} + \delta n_\zeta \right) E_+ - \frac{x}{L_n} E_\xi &= 0, \end{aligned} \quad (10)$$

where the explicit expressions for  $\delta n_\xi$  and  $\delta n_\zeta$  could be found by varying (9). Making the backward transformation with respect to  $\delta n_y$  yields

$$\begin{aligned} \mathbf{E}(\mathbf{r}) &= \exp(in_z^0 z + in_y^0 y) \int_{-\infty}^{\infty} \frac{d\delta n_z}{2\pi} \exp(i\delta n_z z) \times \\ &\quad \int_{-\infty}^{\infty} dy' G(y - y') \exp(-i \tan(\varphi) \delta n_z y') \tilde{\mathbf{E}}(x, y', \delta n_z), \quad \mathbf{r} = (x, y, z) \end{aligned} \quad (11)$$

$$G(y - y') = \frac{\exp(-i(y - y')^2/R^2)}{\sqrt{i\pi} R}, \quad R^2 = 4L_{by}n^{opt}|\sin(\varphi)| \quad (12)$$

where the electric field's components  $\tilde{\mathbf{E}} = (\tilde{E}_+, \tilde{E}_\xi)$  obey the system of equations

$$\begin{aligned} \left( \frac{x}{L_n} - \frac{y}{L_{by}} - 2n^{opt} \cos(\varphi) \delta n_z \right) \tilde{E}_+ + \frac{i}{\sqrt{2}} \left( \frac{\partial}{\partial x} + i \cos \varphi \frac{\partial}{\partial y} \right) n^{opt} \tilde{E}_\xi &= 0 \\ \frac{i}{\sqrt{2}} \left( \frac{\partial}{\partial x} - i \cos \varphi \frac{\partial}{\partial y} \right) n^{opt} \tilde{E}_+ - \frac{x}{L_n} \tilde{E}_\xi &= 0. \end{aligned} \quad (13)$$

Introducing new notations

$$\frac{2^{1/4}}{L_n^{1/2} q_0^{1/4}} \cdot x, \left( \frac{y}{\cos(\varphi)} + 2n^{opt} L_{by} \delta n_z \right) \rightarrow x, y, \partial_{\pm} = \frac{\partial}{\partial x} \pm i \frac{\partial}{\partial y}$$

$$a = \frac{L_n}{L_{by}} \frac{q_0 \cos(\varphi)}{1 + q_0}, \tilde{E}_+, \tilde{E}_{\xi} \rightarrow E_+, E_{\xi}, F = -i \frac{E_+}{\sqrt{1 + q_0}}$$

we read (13) in the compact form

$$\begin{aligned} \partial_+ E_{\xi} + (x - ay) F &= 0 \\ \partial_- F - x E_{\xi} &= 0 \end{aligned} \quad (14)$$

In order to make the first step in analysis of the electric field components behavior in the conversion region, we consider in the next Section WKB solution to the system (14), namely we focus on the quality analysis of the ray trajectory along which the energy of the incident beam of the ordinary (or extraordinary) waves is carried over. Although in the mode conversion region the WKB approximation breaks down and a local full wave equations (14) to be solved, the ray trajectory analysis could be useful.

### 3. Ray Hamiltonian dynamics

The ray representation of the wave field in four dimensional ray phase space  $\mathbf{r} = (x, y)$ ,  $\mathbf{n} = -i\partial/\partial\mathbf{r}$  is governed by Hamilton's equations:

$$\frac{d\mathbf{r}}{ds} = -\frac{\partial D}{\partial \mathbf{n}} \left| \frac{\partial D}{\partial \mathbf{n}} \right|^{-1}, \quad \frac{d\mathbf{n}}{ds} = \frac{\partial D}{\partial \mathbf{r}} \left| \frac{\partial D}{\partial \mathbf{n}} \right|^{-1}, \quad (15)$$

where

$$D(\mathbf{r}, \mathbf{n}) = (n_x^2 + \delta n_y^2 - x(x - ay)) / 2 = 0, \quad (16)$$

is the local dispersion relation and  $s$  denotes the orbit parameter. Since the general picture of the ray behavior in the two-dimensional subspace  $xy$  is of interest, let us re-parameterize  $s \rightarrow \tau$ , where  $d\tau = ds |\partial D/\partial \mathbf{n}|^{-1}$ . Substituting (16) into (15) we obtain

$$\frac{d^2\mathbf{r}}{d\tau^2} = -\frac{\partial U(\mathbf{r})}{\partial \mathbf{r}}, \quad (17)$$

where  $U = x(x - ay)/2$ . The equations constituting (17) are coupled with  $a$  being the coupled coefficient. One can introduce the normal co-ordinates  $\mathbf{r} = (x, y) \rightarrow (u, v)$  reducing the system of equations (17) to two independent ones. The set of linear independent solutions for either of the two is

$$\begin{aligned} u &\sim \exp(\pm \nu \tau), \nu = (\sqrt{1 + a^2} + 1)^{1/2} / \sqrt{2}, \\ v &\sim \exp(\pm i\omega \tau), \omega = (\sqrt{1 + a^2} - 1)^{1/2} / \sqrt{2}. \end{aligned} \quad (18)$$

The expressions (18), which show the projections of Hamiltonian rays on the  $(u, v)$  plane, deserves a few comments. First, note the oscillatory behavior along the  $v$  direction, while the  $u$ -motion displays the influence of a retarding force. Second, due to  $|\nu| \gg |\omega|$

oscillations along the  $v$  direction are not to be clear-cut. Third, we can anticipate the full wave solution to the set of equations (14) could be represented as the superposition of the eigenmodes intrinsic to the confining potential ( $\sim v^2$ ) in the  $v$  direction leading to oscillatory  $v$  motion and the superposition of the linear independent parabolic cylinder functions along  $u$  direction, which proper for the effective potential  $\sim -u^2$ . The full-wave solution to the set of equations (14) is studied in the next Section.

#### 4. An integral representation of solution

We would like to obtain the appropriate particular solution of the system (14) matching to the WKB solution outside the mode conversion region

$$\mathbf{E}|_{u \rightarrow \pm\infty} \sim \mathbf{e} \exp\left(\pm iu^2/2\right) \sum_{p=0}^{\infty} \psi_p(v), \quad (19)$$

where  $\mathbf{e}$  is the polarization vector,  $\psi_p(v)$  is a set of eigen functions to be found,  $\exp(-iu^2/2)$  and  $\exp(iu^2/2)$  correspond to incident O mode (OX conversion) and incident X mode (XO conversion).

With that end in view we introduce two possible functional substitutions [9] providing the identity of the equations constituting (14)

$$F = \left( x \pm \frac{i}{\sqrt{1-ia}} \partial_+ \right) W^\pm \quad (20)$$

$$E_\xi = \left( \mp \frac{i(x-ay)}{\sqrt{1-ia}} + \partial_- \right) W^\pm \quad (21)$$

with  $W^+$  and  $W^-$  being required functions that satisfy the equations

$$\frac{\partial^2 W^\pm}{\partial x^2} + \frac{\partial^2 W^\pm}{\partial y^2} + (x^2 - axy \pm i/\sqrt{1-ia}) W^\pm = 0. \quad (22)$$

Let us use the transformation

$$\begin{aligned} x &= (1 - N^2)^{1/4} (\cos(\psi)u - \sin(\psi)v), \\ y &= (1 - N^2)^{1/4} (\sin(\psi)u + \cos(\psi)v), \end{aligned} \quad (23)$$

where  $\cos(\psi) = (1 + N^2)^{-1/2}$ ,  $\sin(\psi) = N(1 + N^2)^{-1/2}$  and  $N = -(\sqrt{1+a^2} - 1)/a$ , that makes the potential in the brackets in (22) symmetrical

$$\frac{\partial^2 W^\pm}{\partial u^2} + \frac{\partial^2 W^\pm}{\partial v^2} + (u^2 - N^2 v^2 \pm (N + i)) W^\pm = 0. \quad (24)$$

If  $a < > 0$  (see figure 4) then  $N > < 0$ . Seeking the solutions to (24) in the form

$$W^\pm(u, v) = \sum_{p=0}^{\infty} W_p^\pm(u) \phi_p\left(\sqrt{|N|}v\right), \quad (25)$$

where the definition for  $\phi_p(v)$  is given by

$$\phi_p(\sqrt{|N|}v) = \frac{|N|^{1/4}}{(2^p p!)^{1/2} \pi^{1/4}} \exp\left(-N^2 v^2/2\right) H_p\left(\sqrt{|N|}v\right), \quad (26)$$

$$\int_{-\infty}^{\infty} \phi_p\left(\sqrt{|N|}v\right) \phi_k\left(\sqrt{|N|}v\right) dv = \delta_{pk}$$

and  $H_p$  are Hermitian polynomials, we obtain the equation for  $W_p^+$  and  $W_p^-$

$$\frac{\partial^2 W_p^\pm}{\partial u^2} + \left( u^2 - \frac{2\gamma_p^\pm}{\pi} \pm i \right) W_p^\pm = 0, \quad (27)$$

where

$$\gamma_p^\pm = \frac{\pi|N|}{2} \left( 2p + 1 \pm \frac{N}{|N|} \right).$$

Since the properties of  $\gamma_p^\pm$  are important for subsequent analysis we list theirs below expressing its argument  $N$  explicitly

$$\begin{aligned} \gamma_p^+ (N > 0) &= \gamma_p^- (N < 0) = \pi|N|(p+1), \\ \gamma_p^- (N > 0) &= \gamma_p^+ (N < 0) = \pi|N|p, \\ \gamma_{p-1}^+ (N > 0) &= \gamma_p^- (N > 0), \quad \gamma_{p+1}^+ (N < 0) = \gamma_p^- (N < 0). \end{aligned} \quad (28)$$

The solutions  $W_p^+$  and  $W_p^-$  to (27) matching to the WKB solutions (19) for the incident ordinary and extraordinary waves (see Appendix A) are

$$W_p^+(u) = B_p^+ D_{i\gamma_p^+/\pi} \left( \sqrt{2} \exp(i\pi/4)u \right) \quad (29)$$

$$W_p^-(u) = B_p^- D_{-i\gamma_p^-/\pi} \left( -\sqrt{2} \exp(-i\pi/4)u \right), \quad (30)$$

where  $B_p^\pm$  are an arbitrary constants, which we choose so that (20) and (21) fit the incident WKB wave outside the conversion layer. As it is demonstrated in Appendix A  $W_p^+$  and  $W_p^-$  correspond to the incident ordinary and extraordinary waves, respectively. The parameter  $\gamma_p^\pm$  has meaning the length of an evanescence layer (see the equation (A.3)). Its value depends on the mode's number  $\phi_p$  and combination of the parameter's  $N$  sign and the direction of the process (see (28)). That is, first, either of the mode tunnels through an evanescence layer with the efficiency inherent itself, second, the conversion efficiency being in 1D model the invariant under the conversion's direction reversal and the poloidal position of the incident beam changing has no longer the same property in 2D inhomogeneous plasma. Being mentioned for the first time in [8] for the oversimplified plasma model ignoring the poloidal magnetic field and confirmed in [9] for the reasonable plasma model accounting for the poloidal magnetic field  $B_y/B \ll 1$  this property depends entirely on the essential two-dimensional character of the waves.

Inserting (29) and (30) into (20), (21) and (11) after simple algebra we obtain an integral representation of solution to (6)

$$\begin{aligned} E_+(\mathbf{r}) &= \exp(in_z^0 z + in_y^0 y) \sqrt{1 + q_0} \times \\ &\int_{-\infty}^{\infty} \frac{d\delta n_z}{2\pi} \exp(i\delta n_z z) (\pm < I^\pm > + < R^\pm >) \end{aligned} \quad (31)$$

$$\begin{aligned} E_\xi(\mathbf{r}) &= \exp(in_z^0 z + in_y^0 y) \sqrt{1 + ia} \times \\ &\int_{-\infty}^{\infty} \frac{d\delta n_z}{2\pi} \exp(i\delta n_z z) (\mp < I^\pm > + < R^\pm >) \\ &< \dots > = \int_{-\infty}^{\infty} dy' G(y - y') \exp(-i \tan(\varphi) \delta n_z y') (\dots), \end{aligned} \quad (32)$$

where upper signs at  $\langle I^\pm \rangle$  correspond to the incident ordinary wave and lower signs correspond to the incident extraordinary wave. The explicit expressions for  $I^\pm$  and  $R^\pm$  are

$$\begin{aligned} I^\pm &= \sum_{k=0}^{\infty} C_k \phi_k \left( \sqrt{|N|} v \right) D_{\pm i \gamma_k^\pm / \pi} \left( \pm \sqrt{2} \exp(\pm i \pi/4) u \right), \quad N > 0 \\ I^\pm &= \sum_{k=0}^{\infty} C_k \phi_k \left( \sqrt{|N|} v \right) D_{\pm i \gamma_k^\pm / \pi} \left( \pm \sqrt{2} \exp(\pm i \pi/4) u \right), \quad N < 0 \end{aligned} \quad (33)$$

and

$$\begin{aligned} R^+ &= 2|N| \exp \left( i \frac{\pi}{4} \right) \times \\ &\sum_{k=0}^{\infty} C_k k \phi_{k-1} \left( \sqrt{|N|} v \right) D_{i \gamma_k^- / \pi - 1} \left( \sqrt{2} \exp(i \pi/4) u \right), \quad N > 0 \\ R^+ &= -\sqrt{|N|} \exp \left( i \frac{\pi}{4} \right) \times \\ &\sum_{k=0}^{\infty} C_k \phi_{k+1} \left( \sqrt{|N|} v \right) D_{i \gamma_k^- / \pi - 1} \left( \sqrt{2} \exp(i \pi/4) u \right), \quad N < 0, \\ R^- &= 2|N| \exp \left( -i \frac{\pi}{4} \right) \times \\ &\sum_{k=0}^{\infty} C_k k \phi_{k-1} \left( \sqrt{|N|} v \right) D_{-i \gamma_k^+ / \pi - 1} \left( -\sqrt{2} \exp(-i \pi/4) u \right), \quad N < 0 \\ R^- &= -\sqrt{|N|} \exp \left( -i \frac{\pi}{4} \right) \times \\ &\sum_{k=0}^{\infty} C_k \phi_{k+1} \left( \sqrt{|N|} v \right) D_{-i \gamma_k^+ / \pi - 1} \left( -\sqrt{2} \exp(-i \pi/4) u \right), \quad N > 0. \end{aligned} \quad (34)$$

While outside the mode conversion region at  $u \rightarrow \pm\infty$   $\langle I^+ \rangle$  and  $\langle I^- \rangle$  match to the geometrical optics solutions that correspond to the WKB incident and conversed waves (compare the first terms in the r.h.s. of (A.1) and (A.2), (A.6) and (A.7)), the WKB asymptotics of  $\langle R^+ \rangle$  and  $\langle R^- \rangle$  correspond to the WKB wave reflected from the evanescence layer (see (A.5)).

It is possible to obtain asymptotic expansion of the solution for  $\varphi \rightarrow 0$ . For the incident ordinary wave at  $N > 0$  we have

$$\begin{aligned} E_+(\mathbf{r}) &= \sqrt{1 + q_0} \exp \left( i n_z^0 z \right) \int_{-\infty}^{\infty} \frac{d\delta n_z}{2\pi} \sum_{k=0}^{\infty} \exp(i\delta n_z z) C_k \times \\ &(\phi_k(\sqrt{|N|} v) D_{i \gamma_k^- / \pi}(\sqrt{2} \exp(i \pi/4) u) + \\ &2|N| \exp \left( i \frac{\pi}{4} \right) k \phi_{k-1}(\sqrt{|N|} v) D_{i \gamma_k^- / \pi - 1}(\sqrt{2} \exp(i \pi/4) u)) \end{aligned} \quad (35)$$

$$\begin{aligned} E_\xi(\mathbf{r}) &= \sqrt{1 + ia} \exp \left( i n_z^0 z \right) \int_{-\infty}^{\infty} \frac{d\delta n_z}{2\pi} \sum_{k=0}^{\infty} \exp(i\delta n_z z) C_k \times \\ &(-\phi_k(\sqrt{|N|} v) D_{i \gamma_k^- / \pi}(\sqrt{2} \exp(i \pi/4) u) + \\ &2|N| \exp \left( i \frac{\pi}{4} \right) k \phi_{k-1}(\sqrt{|N|} v) D_{i \gamma_k^- / \pi - 1}(\sqrt{2} \exp(i \pi/4) u)). \end{aligned} \quad (36)$$

Last expressions recover the expressions for the electric field components derived in [9] for plasma with  $B_y/B \ll 1$ .

## 5. The asymptotic expressions for the electric field's components

For usual spherical tokamak's configuration O mode cut-off layer and the X mode cut-off layer cross at the small angle, i.e.  $a \ll 1$ . Keeping only terms in (23) being zero and first order quantity with respect to the parameter  $a$  we read it as

$$\begin{aligned} x &\simeq u - av/2, \\ y &\simeq v + au/2, \end{aligned} \quad (37)$$

Then we simplify

$$\begin{aligned} < I^\pm > &\simeq \sum_{k=0}^{\infty} \dots < \phi_k(y/d) >, \\ < R^\pm > &\simeq \sum_{k=0}^{\infty} \dots < \phi_{k\pm 1}(y/d) >, \end{aligned}$$

where  $d = (2^{1/4}(1+q_0)^{1/2}L_{by}^{1/2}\cos(\varphi)^{1/2}) / ((2\pi\lambda)^{1/2}q_0^{1/4})$  and  $y$  is scaled in the units  $\lambda = 2\pi c/\omega$ . Comparing the asymptotic representation of  $D_{\pm i\gamma_p/\pi}$  for the argument  $x \rightarrow \infty$  and asymptotic representation of  $D_{\pm i\gamma_p/\pi}$  for the argument  $x \rightarrow -\infty$  (see Appendix A) we obtain an explicit expressions for the conversion coefficient,  $T_{OX,XO}$ , (in energy) and reflection coefficient,  $R_{OX,XO}$ , where the subscripts  $OX$  and  $XO$  correspond to the direction of the process

$$\begin{aligned} T_{OX} &= \frac{1}{P} \sum_{p=0}^{\infty} \int_{-\infty}^{\infty} \frac{d\delta n_z}{2\pi} |C_p|^2 \exp(-2\gamma_p^\mp), \quad R_{OX} = 1 - T_{OX}, \\ P &= \sum_{p=0}^{\infty} \int_{-\infty}^{\infty} \frac{d\delta n_z}{2\pi} |C_p|^2 \end{aligned} \quad (38)$$

and

$$T_{XO} = \frac{1}{P} \sum_{p=0}^{\infty} \int_{-\infty}^{\infty} \frac{dn_z}{2\pi} |C_p|^2 \exp(-2\gamma_p^\pm), \quad R_{XO} = 1 - T_{XO}. \quad (39)$$

The coefficient  $C_n$  is given by the expression

$$\begin{aligned} C_p &= (2\pi)^2 \times \\ &\int_{-\infty}^{\infty} A(y, z) \exp(-i2\pi(n_z^0 z + \delta n_z z + n_y^0 y)) < \phi_p^*(y/d) > dy dz, \end{aligned} \quad (40)$$

where  $*$  means the complex conjugation,  $A(y, z)$  is given field distribution in the incident beam in the WKB region,  $x$  and  $z$  are scaled in  $\lambda$  and  $P$  is a normalizing coefficient proportional to the beam intensity. The expressions (38) and (39) derived similar to ones obtained in [8, 9] excepting the formula for  $C_p$  given by (40) and deserve one comment. Noting  $T_{OX} \neq T_{XO}$  at the fixed  $a$ , we could read the reciprocal relation for the conversion coefficients in 2D inhomogeneous plasma as

$$T_{OX}(\mathbf{B}) = T_{XO}(-\mathbf{B}), \quad R_{OX}(\mathbf{B}) = R_{XO}(-\mathbf{B}), \quad (41)$$

where the argument  $\mathbf{B}$  is presented explicitly. For the first time the property (41) was mentioned in [8]. In [9] it was proved for plasma with poloidal magnetic field  $B_p/B \ll 1$ .

For illustration, in figure 5 the conversion coefficient,  $T_{OX}$ , of an incident beam with transversal distribution

$$A(y, z) = (\pi\rho^2)^{-1/4} \exp\left(-y^2/(2\rho^2) + in^{opt} \sin(\varphi)y + in^{opt} \cos(\varphi)z\right),$$

calculated with the use of 1D model [4] (dashed curve) and the formula (38) (solid curves) for  $a < 0$  and different  $\varphi$  versus the dimensionless radius,  $\rho_y/\lambda$ , is shown. Calculations are executed under conditions of EBW heating experiment in MAST  $L_n/\lambda = 3$ ,  $L_{by}/\lambda = 70$ ,  $q_0 = 0.7$ ,  $\omega/(2\pi) = 15\text{GHz}$ . Rather strong variation of dependence presented in figure 5 with variation of  $\varphi$  is observed.

## 6. Summary and conclusion

The mode conversion of O mode to X mode have been examined in a spherical tokamak geometry for plasma with a cold plasma dielectric tensor. We have assumed the wavelengths are much shorter than the equilibrium plasma gradient length,  $L_n$ . Thus, we expect WKB approximation to apply except possibly near O-mode cut-off surface or mode conversion layer.

Expanding wave equations in the region near the intersection of O and X mode cut-off surfaces, one finds reduced wave equations appropriate for this region which depends on two coordinates,  $x$  and the poloidal angle  $y$ . We seek the required solution to the set of equations so that it matches to the WKB solution outside the mode conversion region. After functional substitution we have found the integral representations of the required solution.

To the case typical of a spherical tokamak's configuration for which the O mode cut-off layer and the X mode cut-off layer cross at the small angle we have been simplified the obtained integral representations of solution and found the wave fields and the conversion coefficients explicitly.

We have shown that at the fixed poloidal position, i.e. fixed  $a$ , the conversion coefficients obey the reciprocal relation (41) as it was shown earlier in the frame of the model neglecting the poloidal magnetic field [8] and of the model in which the poloidal magnetic field is assumed to be small,  $B_y/B \ll 1$ .

The importance of 2D effects has been demonstrated by the example under the MAST conditions.

## 7. Acknowledgments

The work was supported by RFBR grants 04-02-16404, 06-02-17212

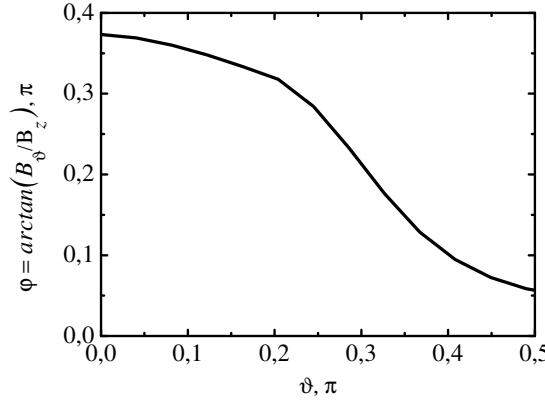


**Figure 1.**  $\varphi = \arctan B_\theta / B_z$  behavior versus the poloidal angle  $\vartheta$  for a typical MAST tokamak discharge

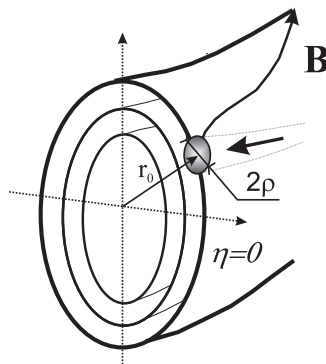


**Figure 2.** Beam with radius  $\rho$  of ordinary polarized electromagnetic waves incident on the O-mode cut-off surface. The co-ordinate  $\mathbf{r}_0$  indicates the position of the beam center on the O-mode cut-off surface

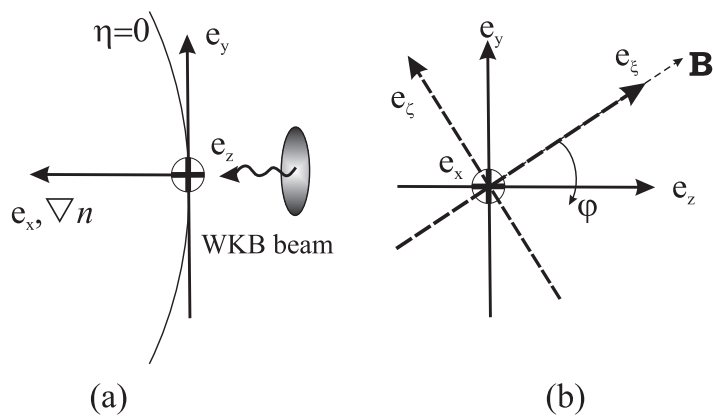


**Figure 3.** Illustration of the co-ordinate systems  $(x, y, z)$  and  $(x, \zeta, \xi)$  used. (a) Two-dimensional subspace  $(xoy)$ ; (b) Two-dimensional subspace  $(yoz)$  with  $\varphi$  being an angle between the magnetic field and the toroidal direction

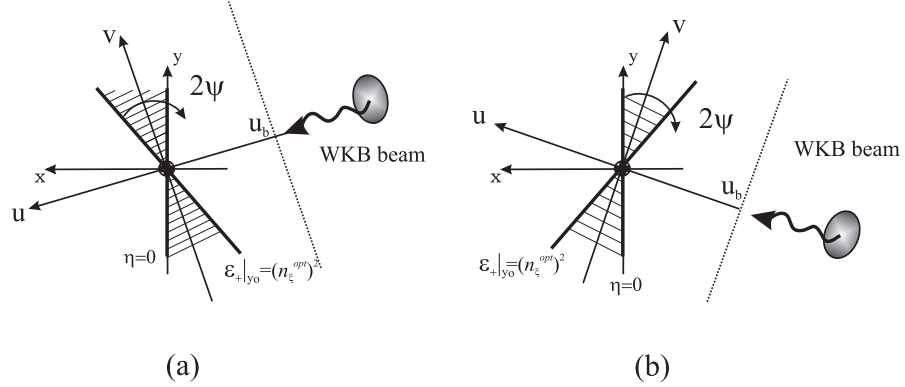


**Figure 4.** Co-ordinate systems  $(x, y)$  and  $(u, v)$  (a)  $a > 0$  ( $N < 0$ ); (b) (a)  $a < 0$  ( $N > 0$ )

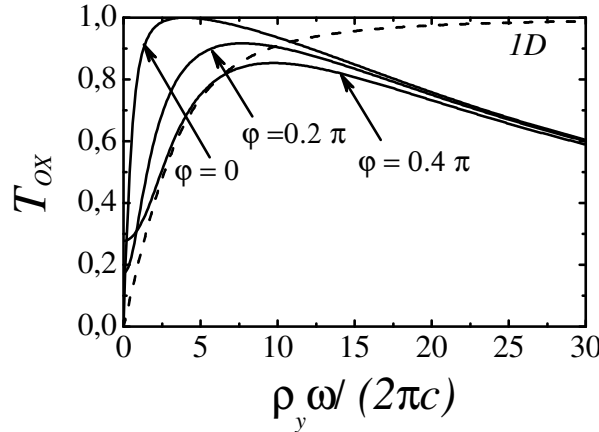


**Figure 5.** The conversion coefficient,  $T_{OX}$ , versus the dimensionless radius,  $\rho_y/\lambda$ , of an incident beam calculated with the use of 1D model [4] (dashed curve) and the formula (38) (solid curves) for  $a < 0$  and different  $\varphi$  under conditions of EBW heating experiment in MAST  $L_n/\lambda = 3$ ,  $L_{by}/\lambda = 70$ ,  $q_0 = 0.7$ ,  $\omega/(2\pi) = 15\text{GHz}$ .

## Appendix A. Asymptotic expressions for the parabolic cylinder functions

We pay our attention to the functions of the parabolic cylinder with different arguments and indices  $D_{i\gamma/\pi}(\sqrt{2} \exp(i\pi/4)u)$  and  $D_{-i\gamma/\pi}(-\sqrt{2} \exp(-i\pi/4)u)$ . Let us begin from asymptotic expressions for the first one at two limits  $u \rightarrow \pm\infty$  which describe the corresponding WKB solutions beyond the conversion layer. When the argument  $u$  tends to  $+\infty$  [12]

$$D_{i\gamma/\pi}(\sqrt{2} \exp(i\pi/4)u) |_{u \rightarrow \infty} \approx (\sqrt{2}u)^{i\gamma/\pi} \exp(-\gamma/4 - iu^2/2), \quad (\text{A.1})$$

while at  $u \rightarrow -\infty$

$$D_{i\gamma/\pi}(\sqrt{2} \exp(i\pi/4)u) |_{u \rightarrow -\infty} \approx (\sqrt{2}u)^{i\gamma/\pi} \exp(3\gamma/4 - iu^2/2) -$$

$$\frac{\sqrt{2\pi}}{\Gamma(-i\gamma/\pi)} \frac{\exp(i3\pi/4)}{(\sqrt{2}u)^{1+i\gamma/\pi}} \exp(\gamma/4 + iu^2/2). \quad (\text{A.2})$$

The second term in (A.2) is much smaller (with factor  $1/u$ ) compared to the first one. Therefore the function  $D_{i\gamma/\pi}(\sqrt{2}\exp(i\pi/4)u)$  in the WKB sense describes the wave approaching an evanescence layer from  $-\infty$  and conversed wave propagating from an evanescence layer to  $\infty$ . Comparing the coefficients at  $\exp(-iu^2/2)$  in (A.1) and (A.2) one obtains the conversion coefficient (in energy) for the wave described by the parabolic cylinder equation

$$T = \exp(-2\gamma). \quad (\text{A.3})$$

Farther we obtain the derivative of the parabolic cylinder function

$$\begin{aligned} \frac{\partial}{\partial u} D_{i\gamma/\pi}(\sqrt{2}\exp(i\pi/4)u) = \\ \frac{2i\gamma}{\pi} \exp(i\pi/4) D_{i\gamma/\pi-1}(\sqrt{2}\exp(i\pi/4)u) - iu D_{i\gamma/\pi}(\sqrt{2}\exp(i\pi/4)u) \end{aligned} \quad (\text{A.4})$$

The first term in the r.h.s. of (A.4), which has the asymptotics [12]

$$\begin{aligned} D_{i\gamma/\pi-1}(\sqrt{2}\exp(i\pi/4)u) |_{u \rightarrow \infty} &\approx O(1/|u|) \\ D_{i\gamma/\pi-1}(\sqrt{2}\exp(i\pi/4)u) |_{u \rightarrow -\infty} &\approx \\ \frac{\sqrt{2\pi}}{\Gamma(1 - i\frac{\gamma}{\pi})} \frac{1}{(\sqrt{2}u)^{i\gamma/\pi}} \exp(\gamma/4 + iu^2/2) &+ O(1/|u|), \end{aligned} \quad (\text{A.5})$$

describes the reflected wave.

Comparing the asymptotic expansions for the parabolic cylinder function  $D_{-i\gamma/\pi}(-\sqrt{2}\exp(-i\pi/4)u)$  [12]

$$\begin{aligned} D_{-i\gamma/\pi}(-\sqrt{2}\exp(-i\pi/4)u) |_{u \rightarrow \infty} &\approx (\sqrt{2}u)^{-i\gamma/\pi} \exp(3\gamma/4) \exp(iu^2/2) - \\ \frac{\sqrt{2\pi}}{\Gamma(i\gamma/\pi)} \frac{\exp(-i3\pi/4)}{(\sqrt{2}u)^{1-i\gamma/\pi}} \exp(\gamma/4) \exp(-iu^2/2). \end{aligned} \quad (\text{A.6})$$

and

$$\begin{aligned} D_{-i\gamma/\pi}(-\sqrt{2}\exp(-i\pi/4)u) |_{u \rightarrow -\infty} &\approx \\ (\sqrt{2}u)^{-i\gamma/\pi} \exp(-\gamma/4) \exp(iu^2/2), \end{aligned} \quad (\text{A.7})$$

we note that it describes the wave which incident on an evanescent layer from  $u \rightarrow \infty$  (see the first term in (A.5)) and propagates from an evanescent layer to the plasma boundary ( $u \rightarrow -\infty$ ) (see (A.6)).

## References

- [1] Laqua H P, Erckmann V, Hartfuss H J and W-A ECRH Group 1997 *Phys. Rev. Lett.* **78** 3467
- [2] Efthimion P C, Hosea J C, Kaita R, Majeski R and Taylor G 1999 *Rev. Sci. Instrum.* **70** 1018
- [3] Shevchenko V, Baranov Y, O'Brien and Saveliev A 2002 *Phys. Rev. Lett.* **89** 265005

- [4] Prienthaler J and Kopecky V 1973 *J. Plasma Physics* **10** 1
- [5] Mjolhus J J 1984 *Plasma Phys.* 31 7
- [6] Tokman M D 1985 *Sov. J. Plasma Phys.* 11 689 (1985)
- [7] Weitzner H 2004 *Phys. Plasmas* **11** 866
- [8] Gospodchikov E D, Shalashov A G, Suvorov E V 2006 *PPCF* **48** 869
- [9] Popov A Yu, Piliya A D 2006 *Plasma Phys. Reports* (to be pub.)
- [10] Cairns R A, Lashmore-Davies C N 2000 *Phys. Plasmas* **7** 4126
- [11] Zharov A A 1984 *Sov. J. Plasma Phys.* 10 642
- [12] *High transcendental functions* (Harry Bateman) (MC Graw-Hill Book Company, Inc, 1953)